Organic Geochemistry 121 (2018) 126–137

Contents lists available at ScienceDirect

Organic Geochemistry

journal homepage: www.elsevier.com/locate/orggeochem

Modelling leaf wax *n*-alkane inputs to soils along a latitudinal transect across Australia

S. Howard [a,*], F.A. McInerney [a], S. Caddy-Retalic [b,c], P.A. Hall [a], J.W. Andrae [a]

[a] University of Adelaide, Sprigg Geobiology Centre and School of Physical Sciences, Australia
[b] University of Adelaide, School of Biological Sciences, Australia
[c] University of Sydney, School of Life and Environmental Sciences, Australia

ARTICLE INFO

Article history:
Received 26 September 2017
Received in revised form 23 March 2018
Accepted 25 March 2018
Available online 29 March 2018

Keywords:
Leaf wax
n-Alkanes
Average chain length
Carbon preference index
Soils
Palaeoecology
Vegetation reconstruction

ABSTRACT

Leaf wax *n*-alkanes provide a valuable palaeoecological proxy, but their interpretation requires an understanding of the scale of temporal and spatial integration in soils. Leaf wax *n*-alkanes are continually deposited into soils directly from local plants as well as from more distant plants via wind or water transport. In addition, *n*-alkanes can persist in soils for thousands of years, and tend to decrease in age with shallower depth. To explore whether the uppermost soils reflect recent leaf fall inputs we compared surface soils and modern vegetation from 20 sites along a transect across Australia. At each site, the three most dominant plant species and a soil sample from the top 3 cm were analysed for *n*-alkane concentration, average chain length (ACL), proportional abundance of C_{33} and C_{29} (Norm33) and carbon preference index (CPI). Chain length distributions differ between trees and grasses, with a higher proportion of C_{29} in trees and C_{33} in grasses. Norm33 in soils correlates with proportional grass to tree cover across the transect. To model *n*-alkane inputs for each site, we calculated a predicted ACL, Norm33 and CPI using the dominant plants at that site, weighted by proportional species cover and *n*-alkane concentration. Predicted ACL, Norm33 and CPI inputs were generally higher than the soils, demonstrating that recent and local inputs do not dominate soil *n*-alkanes at our study sites. Thus, *n*-alkane distributions in surface soils do not correlate with local, current vegetation, but do correlate with proportional grass and tree cover, suggesting they provide a faithful record of large scale ecosystem structure.

1. Introduction

Plant waxes provide critical protection for leaves by limiting non-stomatal water loss from the leaf surface (Eglinton and Hamilton, 1967; Dodd and Poveda, 2003; Jetter and Riederer, 2016), protecting against damage from UV radiation (Shepherd and Wynne Griffiths, 2006; Koch et al., 2009), and resisting fungal infection and herbivory (Eigenbrode and Espelie, 1995; Banthorpe, 2006). Plant waxes contain a range of compounds, including long chain *n*-alkanes, which are non-polar, unbranched, straight-chain hydrocarbons (Eglinton and Hamilton, 1967; Banthorpe, 2006). Long chain-odd-numbered *n*-alkanes (C_{25}–C_{35}) are produced nearly exclusively as part of the waxes of terrestrial plants (Eglinton and Hamilton, 1967). Plants generally produce greater quantities of odd than even chain lengths due to synthesis by sequential elongation or condensation of a C_2 primer, where even-numbered fatty acid chains become decarboxylated to produce odd chain length alkanes (Khan and Kolattukudy, 1974; Shepherd and Wynne Griffiths, 2006). Higher plants produce different distributions of chain lengths that range from C_{25} to C_{35} (Sachse et al., 2004; Pu et al., 2011; Bush and McInerney, 2013). The majority of plant wax *n*-alkanes in soils and sediments should derive from leaves due to the high proportional biomass of leaves, and the high concentrations of *n*-alkanes in leaves relative to other plant organs (Gamarra and Kahmen, 2015). Roots can contribute *n*-alkanes to the soil directly, but their concentration is one or two orders of magnitude less than leaves and thus they are unlikely to be the dominant source of *n*-alkane signals in surface soils (Gamarra and Kahmen, 2015; Angst et al., 2016; Jansen and Wiesenberg, 2017). There is some evidence that insects also produce long-chain *n*-alkanes with an odd-over-even predominance, however their biomass is orders of magnitude less than that of terrestrial plants and their annual *n*-alkane production rate is unquantified, so their contribution to soils and sediments is considered negligible in comparison to plants (Chikaraishi et al., 2012).

Plant lipid biomarkers, such as leaf wax *n*-alkanes, are very common in the sedimentary record, compared to macrofossils

* Corresponding author.
E-mail address: sian.howard@adelaide.edu.au (S. Howard).

https://doi.org/10.1016/j.orggeochem.2018.03.013
0146-6380/

which are comparatively rare. Leaf wax *n*-alkanes are valuable recorders of past vegetation (Eglinton and Eglinton, 2008; Diefendorf and Freimuth, 2017) and can be distinguished from petroleum sources by their odd-over-even predominance (Eglinton and Hamilton, 1967; Yamamoto and Kawamura, 2010). However, to interpret the signatures preserved in sediments, we must understand how sedimentary leaf wax *n*-alkanes reflect the vegetation both temporally and spatially (Diefendorf and Freimuth, 2017).

Direct ^{14}C dating suggests that leaf wax *n*-alkanes can be pre-aged in soils for hundreds to thousands of years prior to remobilisation and transport to lacustrine and marginal marine sediments (Smittenberg et al., 2006; Drenzek et al., 2007; Douglas et al., 2014; Gierga et al., 2016), frequently resulting in highly time-averaged *n*-alkane accumulations. Once buried in sediments, *n*-alkanes can persist for millions of years and have been extracted from sediments from the Cretaceous–Paleogene boundary (Yamamoto et al., 2010), Paleocene–Eocene (Smith et al., 2007), Miocene (Huang et al., 2001) and Holocene (Schwark et al., 2002).

Although *n*-alkanes can persist for thousands of years in deeper subsoils and millions of years in buried sediments, analyses of modern soils demonstrates that more recent *n*-alkane inputs dominate near the soil surface (Angst et al., 2016). Direct ^{14}C dating of *n*-alkanes and soil organic carbon in soils and lake sediments shows increasing age with depth (Huang et al., 1996; Angst et al., 2016; Gierga et al., 2016). Makou et al. (2018) found ^{14}C dating of long, odd-chain *n*-alkanes in a surface soil indicated a pool of pre-aged *n*-alkanes attributed to erosional inputs from adjacent slopes, however the dominant chain length present in the soil, C_{27}, was modern in age and attributed to inputs of fresh leaf waxes from nearby beech trees. Therefore, surface soils appear to be the least time-averaged, and predominantly represent the most recent *n*-alkane inputs.

Leaf fall and breakdown of leaf litter represents direct *n*-alkane deposition to soils (Cranwell, 1981; Lichtfouse et al., 1998), resulting in soil *n*-alkane signatures representative of local sources. Previous work examining the relationship between chain length and biome type showed that the chain length distributions associated with the plants were similar to those in the soils of those respective biomes (Carr et al., 2014). However, leaf wax *n*-alkanes are also readily ablated and wind-dispersed, which would lead soil deposits to represent a regional catchment area (van Gardingen et al., 1991; Gao et al., 2012). Wind-blown *n*-alkanes can travel as far as between continents (Bendle et al., 2007; Yamamoto and Kawamura, 2010; Nelson et al., 2017) and are primarily deposited with particulate matter scrubbed from the atmosphere by precipitation (Meyers and Hites, 1982; Diefendorf and Freimuth, 2017). Similarly, water can transport leaf wax *n*-alkanes long distances via streams, rivers and runoff, either by moving fallen leaves or deposited particulate matter (Rouillard et al., 2016; Diefendorf and Freimuth, 2017). The relative importance of these processes in delivering *n*-alkanes to soils will determine whether soil records represent a regional or more localised vegetation sample (Jansen and Wiesenberg, 2017).

Here, we test the hypothesis that *n*-alkane distributions in surface soils correlate with *n*-alkane distributions of current local vegetation. We sampled a latitudinal transect across Australia to capture a climatically and ecologically diverse set of sites (Fig. 1). The continent-wide transect spans from monsoonal tropics in the north to arid desert in the centre, to the winter-wet Mediterranean climate zone in the south. The biomes sampled include tropical and subtropical grasslands, savannas and shrublands in the north; desert and xeric shrublands in the centre; and Mediterranean shrublands and woodlands in the south (Supplementary Table S1). At each site, we characterised the *n*-alkane abundance and distribution from the three most dominant plant species. At the vast majority of sites, the three dominant species represent the majority of the plant cover (Table 1). While it does not equate directly to biomass, dominant coverage provides us with a reasonable estimate of the dominant *n*-alkane contributors to the surface soils and improves on previous studies that sample plants without respect to their coverage in the landscape. Using the concentration and distribution of *n*-alkanes of the dominant vegetation to account for differences in production, we modelled their inputs to surface soils and compared them to the distributions measured from the soils (top 3 cm). The degree to which local and recent vegetation contributes to soil *n*-alkane signatures will determine how well our modelled inputs match our measured soil *n*-alkane distributions. This comparison provides a direct test of the hypothesis that the leaf wax *n*-alkane signals in surface soils are dominated by local and recent inputs rather than regional and/or long-term inputs. We also examined whether soil *n*-alkane distributions broadly reflect plant cover growth form (e.g., grasses vs trees) at each site. The results constrain the nature of delivery and turnover of *n*-alkane soils across a large and diverse transect, and provide bounds on the range of possible paradigms for the development of *n*-alkane records in soils.

2. Methods

2.1. Sample collection

Soil and plant samples were collected from 20 sites on a north-south transect across Australia (Fig. 1), using the AusPlots Rangelands survey methodology (White et al., 2012). These samples were collected by Australia's Terrestrial Ecosystem Research Network (TERN) and made available for this research. The sites monitored by TERN are permanent plots where baseline surveys of soils and vegetation are conducted as a source of ongoing and long-term ecosystem data for research (White et al., 2012). Sites analysed here were distributed through seven Australian bioregions (See Supplementary Table S1 for descriptions). A single surface soil sample from the middle of each site, taken from a maximum of 3 cm depth (total n = 20), was selected for analysis after having been air dried and stored in calico. Soils were sieved with 1000 and 250 μm sieves to remove large plant material, such as leaves, bark and roots. Particle size percentages were determined using mid-infrared particle size analysis.

Proportional plant species cover and growth form cover was determined from point intercept data obtained from the online Soils2Satellites portal (www.soils2satellites.org.au). At each one hectare site, 1010 points were assessed and all vegetation occurrences were recorded (White et al., 2012). The total number of occurrences for each species and growth form was divided by the total number of vegetation occurrences per site to determine the proportional species cover and growth form (trees, grasses, forbs and shrubs, inclusive of chenopods) cover at each site.

$$\text{Proportional species cover} = \frac{\text{number of species occurrences}}{\text{total vegetation occurrences}} \quad (1)$$

$$\text{Proportional growth form cover} = \frac{\text{number of growth form occurrences}}{\text{total vegetation occurrences}} \quad (2)$$

Leaves from the three most dominant plant species, in terms of proportional species cover, were selected for analysis from each site, except for one site from which the two most dominant were available (total n = 59). The leaves were placed in gauze bags and dried on silica gel. The total proportional species cover that the three most dominant plant species represent ranges from 42 to 99% (Table 1).

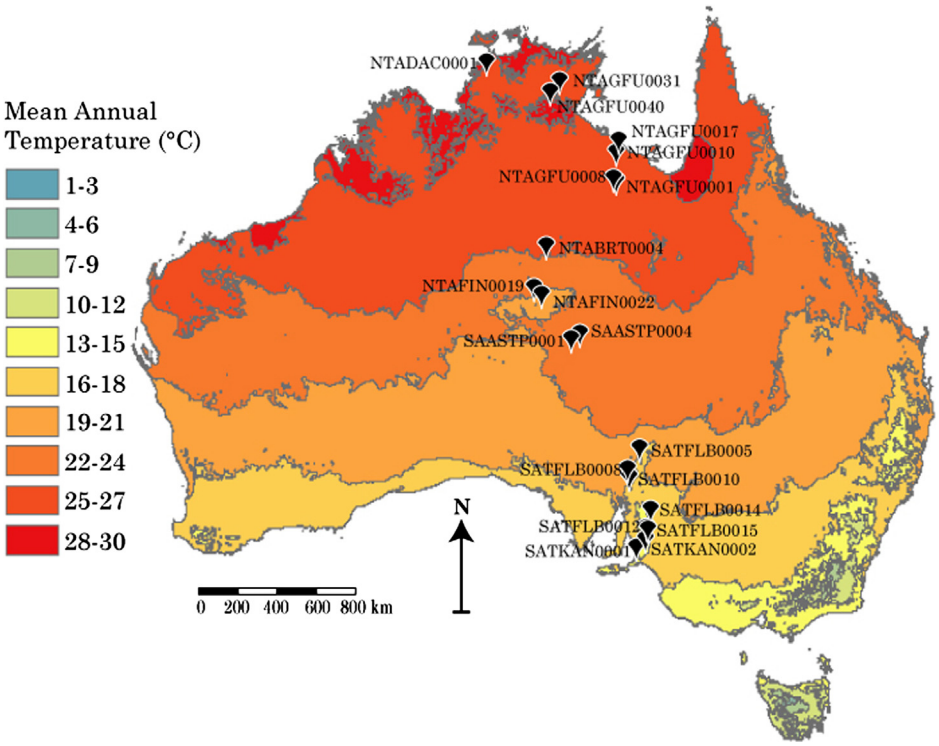

Fig. 1. Location map of selected AusPlots sites (black pins) across Australia with mean annual temperature shown as context. Climate data based on a standard 30-year climatology (1961–1990) and reproduced with permission from Bureau of Meteorology (© Commonwealth of Australia).

2.2. Lipid extraction from plants

Dried plant samples were ground to a fine powder with a mortar and pestle in liquid nitrogen. Lipids were extracted from the ground plant samples in dichloromethane:methanol (DCM:MeOH; 9:1; v:v) in a Soniclean 250TD sonicator. Sample weights ranged from 5.8 to 52.3 mg; with 51 of the 59 plant samples ≥50 mg. Excess solvent was evaporated from the total lipid extract (TLE) under nitrogen gas using a FlexiVap nitrogen blow-down station.

2.3. Lipid extraction from soils

Lipid extraction of the <250 μm soil fraction was conducted using a Thermo Scientific Dionex Accelerate Solvent Extractor (ASE) 350 using DCM:MeOH (9:1, v:v). Samples weights ranged from 4.5 to 26.6 g, with 15 of the 20 soils samples ≥10 mg. The ASE sequence was set to 100 °C with a 12 min preheat, three static cycles of five min, and a rinse volume of 60%. Excess solvent was evaporated from the TLE under nitrogen gas.

2.4. n-Alkane purification

The polar and non-polar fractions of both the plant and the soil TLEs were separated through a short glass column containing silica gel by eluting them with 4 ml of hexane to collect the non-polar, aliphatic hydrocarbon fraction, followed by DCM:MeOH (4 ml, 1:1, v:v) to collect the polar fraction, (modified from Bastow et al., 2007). The aliphatic hydrocarbon fraction was dried under nitrogen gas.

2.5. GC–MS lipid quantification

Quantification of *n*-alkanes was conducted using gas chromatography–mass spectrometry (GC–MS) analysis of the non-polar lipid fraction. Analysis was performed on a Perkin Elmer Clarus 500 GC–MS with the following specifications: The capillary was an SGE CPSil-5MS, 30 m (length) × 0.25 mm (i.d.) × 0.25 μm (phase thickness). The carrier gas was helium with a 1 ml/min constant flow. The injection temperature was 300 °C, with a temperature program of 50 °C (hold 1 min), ramped at 8 °C/min to 340 °C (hold for 7.75 min). Injection was set to 1 μl in either split mode, with a 50:1 split for higher concentration samples, or pulsed splitless for low sample concentrations. Perkin Elmer Turbomass software was used for data interpretation and quantification of *n*-alkane homologues (C_{25} to C_{35}). 1,1′-binaphthyl internal standard was added to each sample at a concentration of 1 μg/mL for quantification. Concentrations of *n*-alkanes were calculated from the response factor of each homologue against the internal standard plotted against a seven point calibration curve prepared and analysed in triplicate using known concentrations of a homologous suite of *n*-alkanes (C_7 to C_{40}) with the same 1 μg/mL 1-1′-binaphthyl internal standard concentration ($r^2 > 0.96$).

2.6. Calculations

Relative abundances of *n*-alkane chain lengths were characterised by calculating average chain length (ACL) (Eglinton and Hamilton, 1967):

$$\mathrm{ACL} = \frac{(25C_{25} + 27C_{27} + 29C_{29} + 31C_{31} + 33C_{33} + 35C_{35})}{(C_{25} + C_{27} + C_{29} + C_{31} + C_{33} + C_{35})} \quad (3)$$

where C_x is the total concentration of each *n*-alkane with *x* carbon atoms.

Carbon preference index (CPI) for each sample was calculated using the equation. Modified from Marzi et al. (1993):

$$\mathrm{CPI} = \frac{\left[\sum_{\mathrm{odd}}(C_{25-33}) + \sum_{\mathrm{odd}}(C_{27-35})\right]}{2\left(\sum_{\mathrm{even}}C_{26-34}\right)} \quad (4)$$

Table 1
Plant species sampled from each site, proportional species cover at each site, *n*-alkane concentration, ACL.

Site	Latitude	Longitude	Dominant plant species 1	Growth form	% Cover	Total μg/mg (C_{25}–C_{35})	ACL	Dominant plant species 2	Growth form	% Cover	Total μg/mg (C_{25}-C_{35})	ACL	Dominant plant species 3	Growth form	% Cover	Total μg/mg (C_{25}-C_{35})	ACL	Total site plant cover (%)
NTABRT 0004	−22.29	133.616	*Acacia aptaneura*	Shrub	54.9	11.84	32.1	*Aristida holathera*	Grass	24	1.33	32.4	*Triodia schinzii*	Grass	7.2	0.38	30.4	85.7
NTADAC 0001	−13.16	130.778	*Sorghum plumosum*	Grass	57.1	0.09	31.8	*Eucalyptus tetrodonta*	Tree	19	0.49	30.3	*Eucalyptus miniata*	Tree	7.8	0.38	29.9	84.3
NTAFIN 0019	−24.36	132.936	*Cenchrus ciliaris*	Grass	67.3	1.98	31.9	*Acacia estrophiolata*	Tree	19	5.63	30.4	*Enchylaena tomentosa*	Grass	2.3	1.37	29.3	88.4
NTAFIN 0022	−24.63	133.452	*Eremophila freelingii*	Shrub	49.6	50.88	30.2	*Enneapogon polyphyllus*	Grass	15	1.58	32.1	*Aristida contorta*	Grass	7.6	1.18	31.7	72
NTAGFU 0001	−18.91	137.069	*Aristida pruinosa*	Grass	16.7	0.58	30.8	*Enneapogon polyphyllus*	Grass	13	0.08	32.1	*Eucalyptus pruinosa*	Tree	13	0.04	27.6	42.22
NTAGFU 0008	−18.79	136.865	*Triodia pungens*	Grass	44.8	1.43	30.8	*Aristida contorta*	Grass	19	7.08	28.5	*Fimbristylis dichotoma*	Grass	14	0.5	32.1	78.2
NTAGFU 0010	−17.9	137.101	*Triodia pungens*	Grass	62.6	1.37	31.1	*Eucalyptus leucophloia*	Tree	36	0.33	30.7	N/A	N/A	N/A	N/A	N/A	99
NTAGFU 0017	−17.35	137.158	*Melaleuca viridiflora*	Shrub	31.2	0.08	28.2	*Chrysopogon fallax*	Grass	9.4	1	30.5	*Schizachyrium fragile*	Grass	7	0.09	31.5	47.6
NTAGFU 0031	−14.13	134.387	*Melaleuca viridiflora*	Shrub	29.9	0.71	31.1	*Schizachyrium pachyarthron*	Grass	28	0.13	31.1	*Petalostigma banksii*	Shrub	9.1	0.05	29.8	66.7
NTAGFU 0040	−14.67	133.845	*Acacia dimidiata*	Shrub	26.7	0.74	31.3	*Heteropogon contortus*	Grass	16	0.27	31.3	*Eucalyptus tectifica*	Tree	9.7	0.06	28.1	52.2
SAASTP 0001	−26.28	134.999	*Maireana aphylla*	Shrub	31	0.66	28.6	*Eragrostis setifolia*	Grass	12	0.25	31.1	*Acacia aneura* var. *tenuis*	Shrub	7.7	3.67	31.7	50.6
SAASTP 0004	−26.09	135.452	*Malvastrum americanum* var. *americanum*	Forb	25.6	1.72	29.6	*Rutidosis helichrysoides* subsp. *helichrysoides*	Forb	19	10.13	31.7	*Sida fubulifera*	Forb	12	5.06	32.2	55.8
SATFLB 0005	−31.32	138.566	*Dodonaea viscosa* subsp. *angustissima*	Shrub	21.8	20.02	28.9	*Eucalyptus flindersii*	Tree	19	0.48	26.7	*Chrysocephalum semipapposum*	Forb	13	5.08	30.5	53.6
SATFLB 0008	−32.32	137.954	*Triodia scariosa*	Grass	45.1	0.13	30.2	*Cassinia laevis*	Shrub	23	1.3	30.3	*Casuarina pauper*	Shrub	12	2.51	31.3	79.6
SATFLB 0010	−32.83	138.033	*Eucalyptus odorata*	Tree	65.1	0.21	26.8	*Rhagodia paradoxa*	Shrub	9.9	0.33	30.2	*Enchylaena tomentosa* var. *tomentosa*	Shrub	6	0.3	30.5	81
SATFLB 0012	−34.88	138.708	*Allocasuarina muelleriana* subsp. *Muelleriana*	Shrub	42	6.16	31.1	*Hibbertia crinita*	Shrub	16	0.14	30.0	*Eucalyptus fasciculosa*	Tree	13	0.04	28.3	70.2
SATFLB 0014	−34.01	138.959	*Eucalyptus odorata*	Tree	32.5	0.32	29.8	*Xanthorrhoea quadrangulata*	Shrub	18	0.22	30.3	*Allocasuarina verticillata*	Shrub	14	4.96	31.0	64.5
SATFLB 0015	−34.93	138.727	*Eucalyptus obliqua*	Tree	60	1.1	28.2	*Lepidosperma semiteres*	Grass	8.3	0.49	31.1	*Hibbertia crinita*	Shrub	6.5	0.6	28.3	74.8
SATKAN 0001	−35.61	138.261	*Eucalyptus baxteri*	Tree	42.5	1.41	29.9	*Lepidosperma semiteres*	Grass	11	0.09	31.5	*Pultenaea involucrata*	Shrub	10	0.37	31.8	63.9
SATKAN 0002	−35.27	138.690	*Eucalyptus obliqua*	Tree	54.7	0.07	29.1	*Lepidosperma semiteres*	Grass	9.1	0.2	31.9	*Hakea rostrata*	Shrub	8.2	0.48	30.4	72

where $\Sigma_{odd}C_{x-y}$ indicates the sum of all concentrations of *n*-alkanes with an odd carbon chain length from *x* to *y* inclusive and $\Sigma_{even}C_{a-b}$ is the sum of concentrations of *n*-alkanes with an even number of carbon chain lengths from *a* to *b* inclusive. Values where CPI > 1.5 were considered to represent an *n*-alkane source of primarily plant origin (Bush and McInerney, 2013).

Predicted soil ACL was calculated as an average of the three dominant plant species' (i = 1, 2, 3) ACL, weighted by both proportional species cover (% $cover_i$) and total concentration from C_{25}–C_{35} ($conc_i$) for each species:

$$\text{Predicted ACL} = \frac{\sum_{i=1}^{3}(\%\ \text{cover}_i \times \text{conc}_i \times \text{ACL}_i)}{\sum_{i=1}^{3}(\%\ \text{cover}_i \times \text{conc}_i)} \quad (5)$$

Predicted soil CPI was calculated as an average of the three dominant plant species' (i = 1, 2, 3) CPI, weighted by both species proportion (% $cover_i$) and concentration ($conc_i$) for each species:

$$\text{Predicted CPI} = \frac{\sum_{i=1}^{3}(\%\ \text{cover}_i \times \text{conc}_i \times \text{CPI}_i)}{\sum_{i=1}^{3}(\%\ \text{cover}_i \times \text{conc}_i)} \quad (6)$$

The proportional abundance of the C_{33} and C_{29} *n*-alkanes, termed Norm33, was calculated modified from Carr et al. (2014):

$$\text{Norm33} = \frac{C_{33}}{(C_{29} + C_{33})} \quad (7)$$

where C_x is the total concentration of each *n*-alkane with *x* carbon atoms.

2.7. Statistical analysis

Welch's t-tests were conducted using KaleidaGraph to examine the differences between the average ACL and Norm33 of the different plant growth forms and the soil. Least squares regression analysis was used to determine the strength of the relationships between the measured *n*-alkanes signals and plant growth form coverage, climate and particle size. Two-sided Kolmogorov-Smirnov tests were conducted using the ks.test function in base R (R Core Team, 2018) and used to compare the relative proportions of different chain lengths in association with different plant growth forms.

2.8. Climate data

Long-term site values for mean annual temperature (MAT), mean annual precipitation (MAP) and annual moisture index (MI), lowest quarter mean MI, highest period radiation and maximum temperature of the hottest month were extracted from ANUCLIM 6.1 layers of a 1960–2014 long term average (Xu and Hutchinson, 2013) through the Atlas of Living Australia (www.ala.org.au).

3. Results

In the plants, C_{31} had the highest concentration in the majority of samples (Fig. 2a, Supplementary Table S2). The ACL for plant samples ranged from 26.7 to 32.4, with a mean value of 30.4 ± 1.4 standard deviation (SD; Table 1). Concentrations of total *n*-alkanes in plants were generally less than <10 μg/mg dry wt, with the exception of three shrubs that ranged up to 50.9 μg/g dry wt (Supplementary Fig. S1).

In the soils, C_{29} had the highest concentration in the majority of samples (Fig. 2b, Supplementary Table S3). The measured ACL in the soils ranged from 27.4 to 30.9, with a mean value of 28.8 ± 0.9 (Table 2).

The average ACL of trees was 28.9 ± 1.4 (n = 13) and was lower and significantly different to that of forbs (31.0 ± 1.2, n = 4, p = 0.02), grasses (31.2 ± 0.9, n = 22, p < 0.0001), and shrubs (30.3 ± 1.2, n = 20, p = 0.005) (Fig. 3a). No other pair-wise comparisons between plant growth form and between plants and soils were statistically distinguishable (p > 0.5) (Fig. 3a).

From north to south, tree cover increased and grass cover decreased (Fig. 4). The measured soil ACL showed a weak but statistically significant positive correlation with grass cover (R^2 = 0.27, p = 0.02) and no relationship with tree cover (R^2 = 0.04, p = 0.4) (Fig. 5a and b).

The average Norm33 of trees was 0.21 ± 0.18 (n = 13) and was lower and significantly different to that of grasses (0.71 ± 0.24, n = 22, p < 0.0001), and shrubs (0.47 ± 0.47, n = 20, p = 0.007), but not distinguishable from that of forbs (0.60 ± 0.28, n = 4, p = 0.2) (Fig. 3b). The Norm33 of grasses was statistically different from shrubs (p = 0.01). No other pairwise comparisons showed statistical difference (p > 0.05) (Fig. 3b).

The measured soil Norm33 showed a weak but statistically significant positive relationship with grass cover (R^2 = 0.21, p = 0.04) and a weak but statistically significant negative relationship with tree cover (R^2 = 0.23, p = 0.03) (Fig. 5c and d).

Kolmogorov-Smirnov tests of leaf wax *n*-alkane distributions indicated that grasses (n = 20) contain significantly higher proportions of C_{33} than trees (n = 13) and shrubs (n = 21); trees contain a significantly higher proportion of C_{29} than grasses; and shrubs are indistinguishable from grasses or trees in terms of the proportion of C_{29} (Fig. 2. and Supplementary Fig. S2).

Plant CPI values ranged from 0.6 to 106.6, with all but one plant showing an odd-over-even carbon number preference (CPI > 1). The one sample that did not have an odd-over-even predominance was *Rhagodia paradoxa*, a chenopod, with a CPI of 0.6. The CPI for the soils ranged from 2.2 to 12.5. This strong odd-over-even predominance indicates that the source of the *n*-alkanes in the soils was from terrestrial higher plants.

In most cases, the predicted soil ACL and Norm33 was higher than the measured soil ACL and Norm33 (Fig. 6a and b). The degree of offset (measured soil-predicted soil) did not correlate with any climate variables (p > 0.05) (Fig. 4 and Supplementary Fig. S3) suggesting that model performance does not vary as a function of climate. Similarly, predicted soil CPI was higher than the measured soil CPI for the majority of sites (Fig. 6c). Particle size analysis revealed no relationship between *n*-alkane concentration, ACL or Norm33 and percentage clay, silt or sand of the soils (Supplementary Fig. S4).

4. Discussion

Long-chain *n*-alkanes extracted from sedimentary archives derived from ancient soils are routinely used as biomarkers for plants, therefore it is vital to understand what these archives represent. Cave sediments, such as Naracoorte Caves in SE Australia, represent a major archive derived largely from terrestrial soils (Macken et al., 2013). Similarly, tectonically active settings, such as the Bighorn Basin and the Siwalik Group preserve paleosols across key intervals of geologic history, such as the Paleocene–Eocene Thermal Maximum and Miocene, respectively (Zaleha, 1997; Smith et al., 2007; Ghosh et al., 2017). To better characterise the nature of these records, we compared *n*-alkane distributions in plants and soils along a transect across Australia to examine whether *n*-alkanes in surface soils are dominated by inputs from the current, local vegetation. We used point intercept data to approximate the proportional species cover of each of the three most dominant species present at a site. We then measured the concentration and distribution of long-chain *n*-alkanes from each of these species and from the surface soils at each site. *n*-Alkane inputs from vegetation are modelled as the cover- and

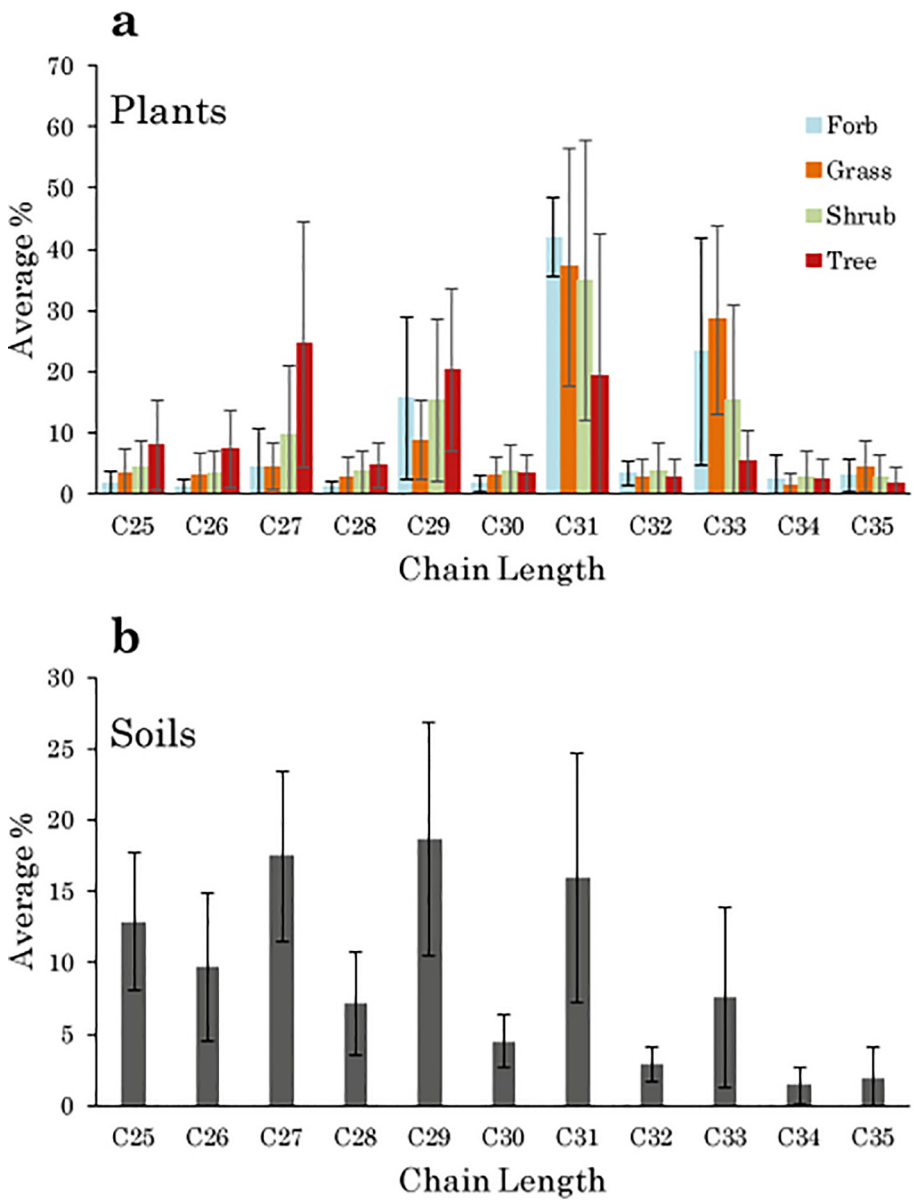

Fig. 2. Relative abundance of *n*-alkanes from (a) plants, separated into their different growth forms, and (b) soils. Distributions displayed as average percentage for each chain length relative to total *n*-alkanes (C_{25}–C_{35}). Error bars represent one standard deviation.

concentration-weighted average of the three most dominant taxa at each site. If local and recent vegetation were the dominant component of surface soil *n*-alkanes, we would expect the modelled *n*-alkane distributions to match those measured in soils. However, the modelled values of both ACL and Norm33 are offset from observed *n*-alkane characteristics, with measured values generally lower than the modelled ones (Fig. 6a and b). The offset between our modelled and observed distributions could be the result of integration of records over larger spatial scales/longer temporal scales than represented by the surveys, could reflect unaccounted fluxes of leaf waxes to soils, or could reflect post-depositional modification. These possibilities are evaluated below.

4.1. Regional vegetation inputs to soils

The modern vegetation survey used here encompasses one hectare plots (0.01 km^2), however, soils may accumulate *n*-alkanes from further afield. Aerosol samples collected from a mid-latitude forest in Germany have shown that their distribution of leaf wax *n*-alkane δD values differs significantly from that of local plants, suggesting that wind dispersal can transport *n*-alkanes across long-distances ranging from hundreds to thousands of kilometres (Nelson et al., 2017). Furthermore, Conte et al. (2003) demonstrated that the isotopic composition of ablated waxes in aerosols collected above a prairie canopy in southern Alberta, Canada, represented a regional scale catchment. Air mass trajectories have shown that wind-blown *n*-alkanes can travel as far as between continents, as well as having a regional or local source (Bendle et al., 2007; Yamamoto and Kawamura, 2010; Nelson et al., 2017). While *n*-alkanes in the atmosphere necessarily represent wind-blown aerosols, it is unclear whether in soils the aerosol deposition represents a significant contribution in comparison to local direct leaf fall. The offset observed here between measured and modelled *n*-alkane distributions may indicate that the signals recorded in the surface soils are integrating across a larger area than the one hectare survey plot.

Table 2
Soil samples from each site. Predicted CPI and ACL modelled from the plants.

Site	Total μg/mg (C_{25}-C_{35})	Measured CPI	Predicted CPI	Measured ACL	Predicted ACL
NTABRT 0004	0.017	6.0	14.6	30.9	32.1
NTADAC 0001	0.341	1.3	3.3	27.8	30.7
NTAFIN 0019	0.0004	5.8	23.9	29.6	31.2
NTAFIN 0022	0.224	1.1	1.9	27.9	30.2
NTAGFU 0001	0.006	3.6	3.1	30.0	30.8
NTAGFU 0008	0.003	3.6	14.3	29.8	29.4
NTAGFU 0010	0.028	6.1	42.8	29.9	31.1
NTAGFU 0017	0.044	3.4	4.7	28.1	30.1
NTAGFU 0031	0.002	2.2	2.1	29.3	31.1
NTAGFU 0040	0.022	4.5	4.7	29.4	31.3
SAASTP 0001	0.125	1.4	13.2	27.4	30.4
SAASTP 0004	0.002	1.2	8.2	28.2	31.5
SATFLB 0005	0.16	2.1	3.3	28.2	29.0
SATFLB 0008	0.113	1.9	4.6	28.5	30.8
SATFLB 0010	0.141	1.9	2.2	28.2	27.7
SATFLB 0012	0.001	1.8	31.6	28.2	31.1
SATFLB 0014	0.005	2.5	48.7	29.0	30.8
SATFLB 0015	0.005	4.9	4.8	27.8	28.4
SATKAN 0001	0.339	6.4	5.6	28.6	30.0
SATKAN 0002	0.007	3.3	36.3	28.1	30.1

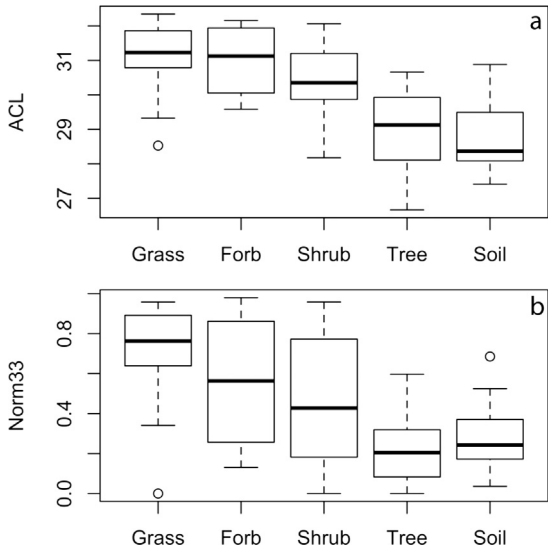

Fig. 3. (a) Boxplots of ACL values for plants, grouped by plant growth form, and soils. (b) Boxplots of Norm33 values for plants, grouped by plant growth form, and soils. Boxes represent 50% of the data, with the median shown by the line. Whiskers indicate lower and upper quartiles.

We observe a systematically shorter chain length distribution in the surface soils than that of the local plant community, which could result if regional aerosol or water borne inputs have shorter chain length distributions. Our results show that of all the growth forms, trees have the shortest average chain length (Fig. 3a). Therefore, if trees from outside of the hectare plots are contributing significantly to soils, this would explain the systematic offset between the local plant community and the surface soils. We hypothesize that trees may be overrepresented in the surface soils relative to other plant types due to their height in the landscape making them more susceptible to ablation by wind as compared to plants lower in stature, such as small shrubs and grasses.

4.2. Time averaging of n-alkane distributions in soils

The model uses the plants surveyed at the time of soil collection as the basis for the vegetation inputs to examine whether leaf waxes in surface soils are dominated by recent vegetation. However, *n*-alkanes can accumulate in soils over hundreds or thousands of years and then be re-mobilised and deposited with younger lacustrine and marine sediments (Smittenberg et al., 2006; Drenzek et al., 2007; Douglas et al., 2014; Gierga et al., 2016). If the *n*-alkanes in the surface soils accumulated over thousands of years, the standing plant community would be a poor predictor of soil *n*-alkane distributions because the dominant vegetation and climate across Australia have changed radically over this time (Hope, 2017). Over the course of the Late Pleistocene into the Holocene, variable but increasing aridity has resulted in a shift from forested to herbaceous vegetation in the Western Plains of Victoria (Edney et al., 1990) and an increase in the dominance of eucalypt dominated grassy woodlands in the last 5000 years in mainland SE Australia (Kershaw et al., 1991). More recently, vegetation has changed since European settlement. Australia's vegetation prior to European settlement had greater plant cover than today, with forests and woodlands in greater abundance (COAG Standing Council on Environment and Water, 2012). Past ecosystems with different *n*-alkane contributors would have produced different *n*-alkane distributions in soils. Environmental changes over the lifetime of the soil would cause a difference between the modern plant community and the temporally integrated soils. This would prevent soils from providing annual or decadal records, but not impact on using soils as recorders of long-term vegetation over centuries to millennia.

4.3. Unconstrained fluxes from plants to soils

Despite accounting for the relative abundances of the plants and differences in *n*-alkane concentration among the plants, we are unable to quantify the actual flux of *n*-alkanes from the plants to the surface soils. The flux can vary with the rate of litter fall, which is a function of leaf lifespan (Wright and Cannon, 2001), or with wax turnover rates within leaves due to physical removal (e.g., by wind ablation and herbivore removal and subsequent deposition) and regeneration of waxes (Koch et al., 2004). Leaf lifespan represents the duration of photosynthetic return to the plant and is balanced against the cost of producing greater leaf mass area (Wright et al., 2004). A global study of leaf economics has shown that in general plants that grow in arid conditions with higher mean annual temperature tend to have longer leaf lifespans (Wright et al., 2004). Our transect represents a broad range of climatic conditions, ranging from monsoonal tropics in the north, to

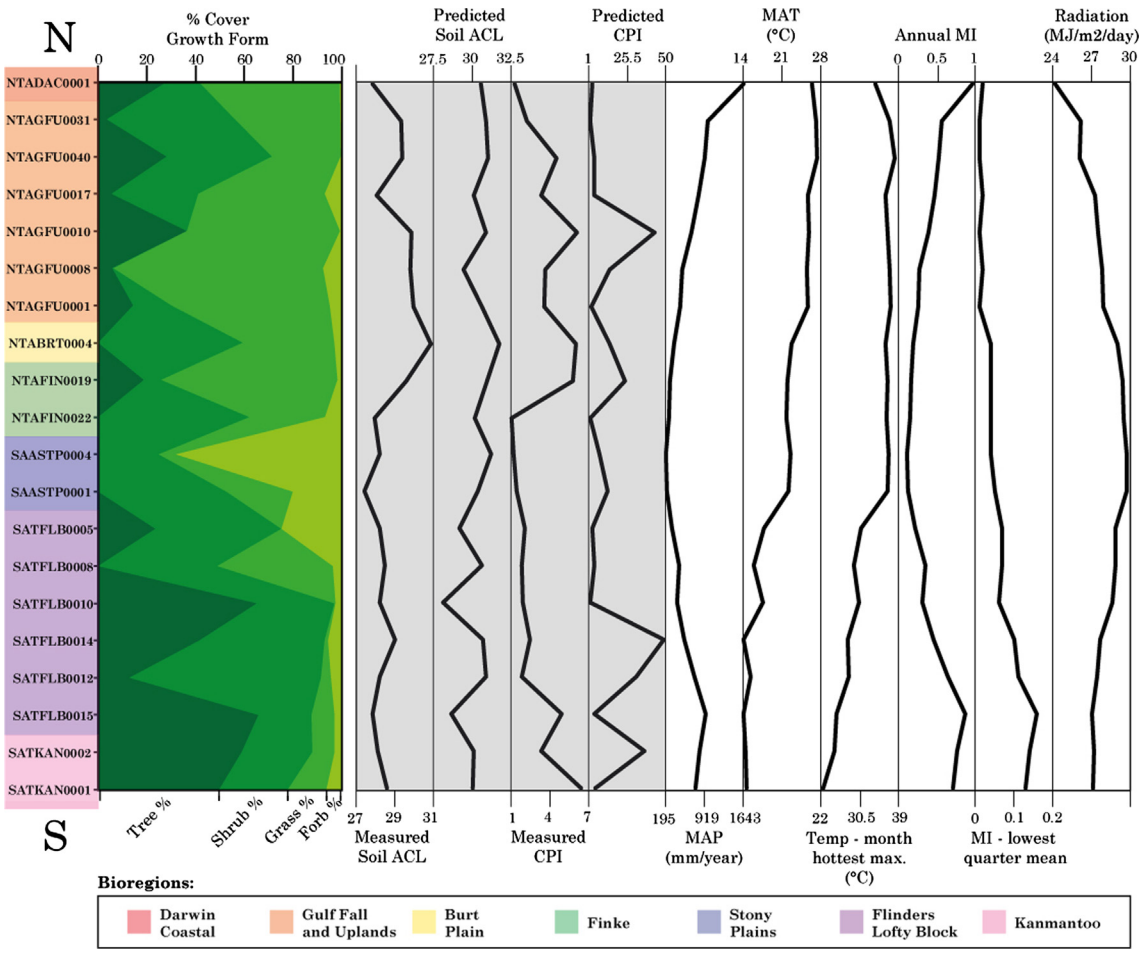

Fig. 4. Proportional coverage of the plant growth forms at each site compared to the measured and predicted soil ACL (unitless), the measured and predicted soil CPI (unitless), MAP, MAT, maximum temperature of the hottest month, annual and lowest quarter mean MI (unitless) and highest period of radiation for each site. Site bioregions (see Supplementary Table S1 for descriptions) indicated by colour bar.

arid central deserts, to winter rainfall in the south. These climatic differences are likely to contribute to variations in both leaf lifespan and the flux of litter to surface soils across the transect. Furthermore, the seasonal dominance of some annual species (e.g., *Sorghum* spp.) would lead to intra-annual variability in both local and regional *n*-alkane inputs. Similarly, differences in the rate of wax production and replacement within a leaf, particularly in rarer species, would result in inputs to surface soils that are not proportional to the standing vegetation composition and concentration. Our inability to constrain fluxes from plants to surface soils would contribute to the spread in the offset between modelled and measured values. However, it is unlikely to explain the systematic overestimates in modelled ACL and CPI.

4.4. Post-depositional modification

Our model tests the local, modern day inputs of *n*-alkanes, but does not measure the fate of these compounds once they have been deposited in the soils. In theory, post-depositional modification to the *n*-alkanes could alter the chain length distributions in soils. In Australian soils, carbon content of soils is positively correlated with precipitation and negatively correlated with temperature; high pH and high clay content also facilitate preservation (Oades, 1988; Carvalhais et al., 2014). Soil particle size is considered to play an important role in turnover of carbon, with decreasing carbon content and increasing carbon turnover rates in soils of increasing particle size (Cayet and Lichtfouse, 2001; Quenea et al., 2004; Quénéa et al., 2006). However, our study finds no correlation between particle size and *n*-alkane concentration or distribution (Supplementary Fig. S4).

At a global scale, organic matter turnover times vary across different biomes with shorter turnover times in tropical forests, savannahs and grasslands and longer turnover times in temperate forests, grasslands and shrublands (Carvalhais et al., 2014). We expect that variation in edaphic conditions could result in differential preservation potential of lipids. Bull et al. (2000) found an increase in *n*-alkane concentrations in soils with a higher pH and Pisani et al. (2015) found that soil warming resulted in a decrease in aliphatic lipid concentrations in the soil mineral horizon. Wang et al. (2017a) similarly find a decrease in concentration of *n*-alkanes with experimental heating at diagenetic temperatures ranging from 60 to 300 °C, as well as a decrease in ACL over time. However, due to our use of surface soils at a depth of only 3 cm, we expect temperatures to be significantly lower than in this experiment, and thus diagenetic effects to be minimised. Validated modelling of soil temperatures across Australia at 5 cm depths, a depth at which air temperature is the primary driver of the subsequent soil temperature, showed that even at extreme maximum temperatures of the year and day, soil temperature did not exceed 40 °C (Horton, 2012). In addition, if variations in climate controlled the degree of post-depositional modification, we would expect the offset between modelled and measured values to vary with climate. However, we find the degree of offset between our modelled and measured ACL does not correlate with temperature or precipitation

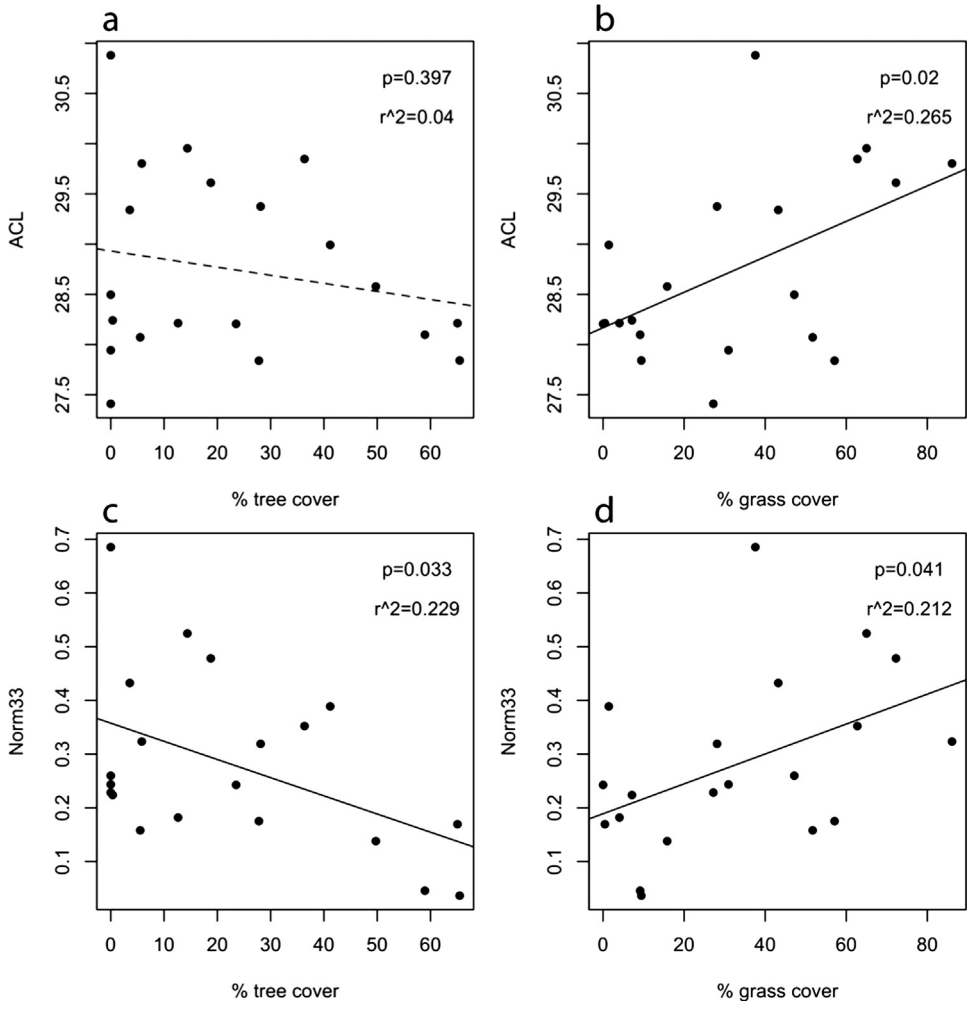

Fig. 5. Plots showing the relationship between ACL measured in the soils vs (a) the percentage of tree cover and, (b) the percentage of grass cover; plots showing the relationship between Norm33 measured in the soils vs (c) the percentage of tree cover and, (d) the percentage of grass cover. Black solid trend lines indicate a significant relationship ($p < 0.05$), a dashed trendline indicates a non-significant relationship ($p > 0.05$).

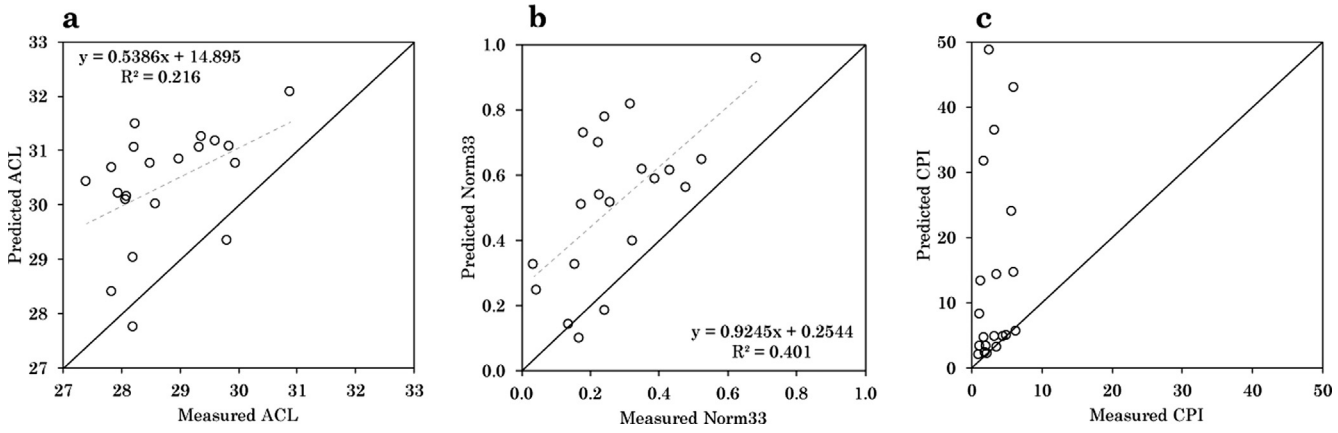

Fig. 6. Predicted vs measured soil (a) ACL, (b) Norm33 and (c) CPI. Prediction represents a concentration- and cover-weighted average of three most dominant plants at each site. The grey dashed line represents the trend. The black 1:1 line is shown for comparison.

(Supplementary Fig. S3). Thus, there is no evidence for climate-driven differences in post-depositional processing in our dataset.

Litterbag studies have explored the effects of microbial degradation on leaf waxes, but the effects varied among studies. Zech et al. (2011) find a decrease in concentration of odd, long-chain *n*-alkanes, as well a decrease in their odd-over-even predominance in a leaf litter bag experiment over 27 months which they interpret as a degradation signal. Similarly, our results show that overall the soils have a lower CPI than do the modelled plant inputs (Fig. 6c), which may indicate that degradation processes impact *n*-alkane

signals in the soil. In contrast, Nguyen Tu et al. (2017) noted that degradation processes resulted in a decrease in concentration of *n*-alkanes in a two-year litterbag study of beech leaves submerged in a pond, but did not result in a change to CPI, nor ACL. Additionally, Celerier et al. (2009) found that the longer chain lengths were not preferentially removed with depth in a soil profile of a long-term field experiment in France and show high resistance to microbial degradation. There is some evidence that differences in soil conditions may have an effect, where Li et al. (2017) found a small change to ACL of buried leaves at one of sites, but not at the other, with a different soil type. This evidence suggests that the ACL is not drastically altered by degradation processes in the soils, but that instead the odd-over-even predominance may vary in soils significantly as a result of degradation. As such, post-depositional modification is not a likely explanation for the ACL offset between the plants and surface soils.

4.5. Vegetation type and climatic effects on n-alkane distribution

A meta-analysis of plants from around the globe showed that in general grasses do not have longer ACL than woody vegetation (Bush and McInerney, 2013). However, within Africa, C4 monocots (grasses and sedges) produce more C_{33} than C3 plants, and C3 plants tend to produce more C_{29} than C4 monocots (Garcin et al., 2014). Similarly, in Australia, the grasses, which are predominantly C4, produce proportionally more C_{33} and had significantly longer ACL than trees (Fig. 3); trees produced statistically more C_{29}, and had a shorter ACL than grasses (Fig. 3). Shrubs and forbs produced a widely varying range of chain lengths (Fig. 3). Plant coverage effects are also evident in the soils. We find statistically significant ($p < 0.05$) correlations between percent grass cover with both Norm33 and ACL and between percent tree cover and Norm33 (Fig. 5). Similarly variations between biomes are seen in sediments from the southwest African continental margin, with longer chain lengths associated with savannahs, compared to shorter chain lengths in rainforests (Rommerskirchen et al., 2006). Carr et al. (2014) found that although there was considerable individual plant variability in the succulent karoo and fynbos biomes of South Africa, the succulent karoo was associated with longer maximum chain lengths than the fynbos, and these longer chain lengths were mirrored in the soils.

An alternative hypothesis for the cause of plant type differences observed here is that chain length distributions could be directly influenced by climate (Bush and McInerney, 2013, 2015). Evidence of correlations between ACL and climate (e.g., temperature, relative humidity) have been found in North America (Tipple and Pagani, 2013; Bush and McInerney, 2015), Italy (Leider et al., 2013), on the Tibetan Plateau (Jia et al., 2016) and in Australia (Hoffmann et al., 2013). We found no relationship between any climate variables and the ACL of plants or soils, testing both climatic extremes and annual means of both temperature and precipitation (Fig. 4, Supplementary Figs. S5 and S6). This is similar to the findings of Wang et al. (2017b), who did not find a strong relationship with temperature and ACL in soils across a >1000 km transect in SW China. Plant type appears to be a greater determinant of ACL than climate in this study. Carr et al. (2014), found that climate was only very weakly correlated with ACL, while there were clear differences between growth forms. Phylogenetic constraints on leaf wax concentration and distribution was shown among conifers (Diefendorf et al., 2015) and may play a role in constraining responses to climate in other groups as well.

4.6. Evaluation of factors influencing soil n-alkane signatures

Our results suggest that soil *n*-alkanes are not dominantly from local and recent vegetation at the sites examined in this study. Moreover, a greater influence of trees from more distant, or previous plant communities could cause shorter ACL in the soils than that observed in modern, local vegetation. Our inability to account for the flux of waxes from the local plants into the soils is noteworthy, but unlikely to result in systematic overestimates by the models. Post-depositional microbial modification may contribute to the reduction in CPI in soils compared to plants, but is unlikely to affect ACL. The offsets between the modelled and measured ACL and Norm33 most likely reflect that soils integrate over larger spatial and/or temporal scales than those sampled by our plant survey. The correspondence between plant cover type (percent grass or percent trees) and *n*-alkane distributions (Norm33, ACL) in soils suggests that soil *n*-alkanes faithfully record larger scale ecosystem features, rather than localised plant communities.

4.7. Implications for palaeoecology

Our results show that while we can be confident that the *n*-alkanes found in the surface soils are of a terrestrial plant origin due to their odd-over-even predominance. We suggest that the leaf waxes in the soils represent a spatially and/or temporally integrated signal. A distinct benefit for palaeoecology is that *n*-alkanes in soils should not be susceptible to microclimates, spatial heterogeneity of vegetation, or short term changes in vegetation due to interannual variability. The correspondence of *n*-alkane distributions in soils with plant cover type (grass or tree) suggests that information on vegetation structure is preserved in soils. Although we detect degradation processes occurring in the soils, with a decrease in soil CPI relative to the vegetation, we do not expect that the ACL of the soils is affected by degradation based on the results of previous studies, however further work to investigate this at greater depth is necessary.

5. Conclusions

Characterising the temporal and spatial scale of inputs of *n*-alkanes from plants to surface soils allows us to better understand what we are measuring when analysing these compounds. Our results show an offset between the modelled signals based on current and local vegetation, and the measured signals in the soils. This offset allows us to reject the hypothesis of recent and local source, and indicates spatial and/or temporal averaging of inputs into the soils. We further suggest that trees are the likely source of the shorter ACL observed in the soils, due to their elevation in the landscape, making them potentially more susceptible to wind ablation than lower-statured species, and due to their greater presence in Australia's pre-European settlement as compared to today. Vegetation cover type (percent grass or percent tree) correlates with surface soil *n*-alkane distributions (Norm33), suggesting that large-scale features of vegetation structure are preserved in soil *n*-alkanes. The signals we observe in sedimentary records are likely to reflect a regional, time-averaged signal that is not heavily susceptible to short-term variability or small-scale spatial heterogeneity in climate.

Acknowledgements

The authors thank the Terrestrial Ecosystem Research Network, for providing the samples and vegetation cover data used in this study. Thanks also to Kristine Nielson for assistance in the lab, Emrys Leitch for help with vegetation data and David McInerney for statistical advice. We also wish to thank three anonymous reviewers for their helpful comments. Funding was provided by the Australian Research Council to FAM (FT110100793, DP130104314). This research is also supported by Australian

Government Research Training Program (RTP) Scholarships to SH, SC-R and JWA.

Appendix A. Supplementary material

Supplementary data associated with this article can be found, in the online version, at https://doi.org/10.1016/j.orggeochem.2018.03.013.

Associate Editor—**Myrna Simpson**

References

Angst, G., John, S., Mueller, C.W., Kögel-Knabner, I., Rethemeyer, J., 2016. Tracing the sources and spatial distribution of organic carbon in subsoils using a multi-biomarker approach. Scientific Reports 6. https://doi.org/10.1038/srep29478.

Banthorpe, D.V., 2006. Natural Occurrence, Biochemistry and Toxicology, Alkanes and Cycloalkanes. John Wiley & Sons, Ltd, pp. 895–926.

Bastow, T.P., van Aarssen, B.G.K., Lang, D., 2007. Rapid small-scale separation of saturate, aromatic and polar components in petroleum. Organic Geochemistry 38, 1235–1250.

Bendle, J., Kawamura, K., Yamazaki, K., Niwai, T., 2007. Latitudinal distribution of terrestrial lipid biomarkers and *n*-alkane compound-specific stable carbon isotope ratios in the atmosphere over the western Pacific and Southern Ocean. Geochimica et Cosmochimica Acta 71, 5934–5955.

Bull, I.D., van Bergen, P.F., Nott, C.J., Poulton, P.R., Evershed, R.P., 2000. Organic geochemical studies of soils from the Rothamsted classical experiments—V. The fate of lipids in different long-term experiments. Organic Geochemistry 31, 389–408.

Bush, R.T., McInerney, F.A., 2013. Leaf wax *n*-alkane distributions in and across modern plants: implications for paleoecology and chemotaxonomy. Geochimica et Cosmochimica Acta 117, 161–179.

Bush, R.T., McInerney, F.A., 2015. Influence of temperature and C4 abundance on *n*-alkane chain length distributions across the central USA. Organic Geochemistry 79, 65–73.

Carr, A.S., Boom, A., Grimes, H.L., Chase, B.M., Meadows, M.E., Harris, A., 2014. Leaf wax *n*-alkane distributions in arid zone South African flora: environmental controls, chemotaxonomy and palaeoecological implications. Organic Geochemistry 67, 72–84.

Carvalhais, N., Forkel, M., Khomik, M., Bellarby, J., Jung, M., Migliavacca, M., Mu, M., Saatchi, S., Santoro, M., Thurner, M., Weber, U., Ahrens, B., Beer, C., Cescatti, A., Randerson, J.T., Reichstein, M., 2014. Global covariation of carbon turnover times with climate in terrestrial ecosystems. Nature 514, 213–217.

Cayet, C., Lichtfouse, E., 2001. $\delta^{13}C$ of plant-derived *n*-alkanes in soil particle-size fractions. Organic Geochemistry 32, 253–258.

Celerier, J., Rodier, C., Favetta, P., Lemee, L., Ambles, A., 2009. Depth-related variations in organic matter at the molecular level in a loamy soil: reference data for a long-term experiment devoted to the carbon sequestration research field. European Journal of Soil Science 60, 33–43.

Chikaraishi, Y., Kaneko, M., Ohkouchi, N., 2012. Stable hydrogen and carbon isotopic compositions of long-chain (C_{21}–C_{33}) *n*-alkanes and *n*-alkenes in insects. Geochimica et Cosmochimica Acta 95, 53–62.

COAG Standing Council on Environment and Water, 2012. Australia's Native Vegetation Framework. Australian Government, Department of Sustainability, Environment, Water, Population and Communities, Canberra.

Conte, M.H., Weber, J.C., Carlson, P.J., Flanagan, L.B., 2003. Molecular and carbon isotopic composition of leaf wax in vegetation and aerosols in a northern prairie ecosystem. Oecologia 135, 67–77.

Cranwell, P.A., 1981. Diagenesis of free and bound lipids in terrestrial detritus deposited in a lacustrine sediment. Organic Geochemistry 3, 79–89.

Diefendorf, A.F., Freimuth, E.J., 2017. Extracting the most from terrestrial plant-derived *n*-alkyl lipids and their carbon isotopes from the sedimentary record: a review. Organic Geochemistry 103, 1–21.

Diefendorf, A.F., Leslie, A.B., Wing, S.L., 2015. Leaf wax composition and carbon isotopes vary among major conifer groups. Geochimica et Cosmochimica Acta 170, 145–156.

Dodd, R.S., Poveda, M.M., 2003. Environmental gradients and population divergence contribute to variation in cuticular wax composition in Juniperus communis. Biochemical Systematics and Ecology 31, 1257–1270.

Douglas, P.M.J., Pagani, M., Eglinton, T.I., Brenner, M., Hodell, D.A., Curtis, J.H., Ma, K. F., Breckenridge, A., 2014. Pre-aged plant waxes in tropical lake sediments and their influence on the chronology of molecular paleoclimate proxy records. Geochimica et Cosmochimica Acta 141, 346–364.

Drenzek, N.J., Montluçon, D.B., Yunker, M.B., Macdonald, R.W., Eglinton, T.I., 2007. Constraints on the origin of sedimentary organic carbon in the Beaufort Sea from coupled molecular ^{13}C and ^{14}C measurements. Marine Chemistry 103, 146–162.

Edney, P.A., Kershaw, A.P., De Deckker, P., 1990. A late Pleistocene and Holocene vegetation and environmental record from Lake Wangoom, Western Plains of Victoria, Australia. Palaeogeography, Palaeoclimatology, Palaeoecology 80, 325–343.

Eglinton, G., Hamilton, R.J., 1967. Leaf epicuticular waxes. Science 156, 1322–1335.

Eglinton, T.I., Eglinton, G., 2008. Molecular proxies for paleoclimatology. Earth and Planetary Science Letters 275, 1–16.

Eigenbrode, S.D., Espelie, K.E., 1995. Effects of plant epicuticular lipids on insect herbivores. Annual Review of Entomology 40, 171–194.

Gamarra, B., Kahmen, A., 2015. Concentrations and δ^2H values of cuticular *n*-alkanes vary significantly among plant organs, species and habitats in grasses from an alpine and a temperate European grassland. Oecologia 178, 981–998.

Gao, L., Burnier, A., Huang, Y., 2012. Quantifying instantaneous regeneration rates of plant leaf waxes using stable hydrogen isotope labeling. Rapid Communications in Mass Spectrometry 26, 115–122.

Garcin, Y., Schefuß, E., Schwab, V.F., Garreta, V., Gleixner, G., Vincens, A., Todou, G., Séné, O., Onana, J.-M., Achoundong, G., Sachse, D., 2014. Reconstructing C3 and C4 vegetation cover using *n*-alkane carbon isotope ratios in recent lake sediments from Cameroon, Western Central Africa. Geochimica et Cosmochimica Acta 142, 482–500.

Ghosh, S., Sanyal, P., Kumar, R., 2017. Evolution of C4 plants and controlling factors: insight from *n*-alkane isotopic values of NW Indian Siwalik paleosols. Organic Geochemistry 110, 110–121.

Gierga, M., Hajdas, I., van Raden, U.J., Gilli, A., Wacker, L., Sturm, M., Bernasconi, S. M., Smittenberg, R.H., 2016. Long-stored soil carbon released by prehistoric land use: evidence from compound-specific radiocarbon analysis on Soppensee lake sediments. Quaternary Science Reviews 144, 123–131.

Hoffmann, B., Kahmen, A., Cernusak, L.A., Arndt, S.K., Sachse, D., 2013. Abundance and distribution of leaf wax *n*-alkanes in leaves of Acacia and Eucalyptus trees along a strong humidity gradient in northern Australia. Organic Geochemistry 62, 62–67.

Hope, G.S., 2017. Quaternary vegetation. In: Hill, R.S. (Ed.), History of the Australian Vegetation: Cretaceous to Recent. University of Adelaide Press, pp. 368–389.

Horton, B., 2012. Models for estimation of hourly soil temperature at 5 cm depth and for degree-day accumulation from minimum and maximum soil temperature. Soil Research 50, 447–454.

Huang, Y., Bol, R., Harkness, D.D., Ineson, P., Eglinton, G., 1996. Post-glacial variations in distributions, ^{13}C and ^{14}C contents of aliphatic hydrocarbons and bulk organic matter in three types of British acid upland soils. Organic Geochemistry 24, 273–287.

Huang, Y., Street-Perrott, F.A., Metcalfe, S.E., Brenner, M., Moreland, M., Freeman, K. H., 2001. Climate change as the dominant control on glacial-interglacial variations in C3 and C4 plant abundance. Science 293, 1647–1651.

Jansen, B., Wiesenberg, G.L.B., 2017. Opportunities and limitations related to the application of plant-derived lipid molecular proxies in soil science. Soil 3, 211–234.

Jetter, R., Riederer, M., 2016. Localization of the transpiration barrier in the epi- and intracuticular waxes of eight plant species: water transport resistances are associated with fatty acyl rather than alicyclic components. Plant Physiology 170, 921–934.

Jia, Q., Sun, Q., Xie, M., Shan, Y., Ling, Y., Zhu, Q., Tian, M., 2016. Normal alkane distributions in soil samples along a Lhasa-Bharatpur transect. Acta Geologica Sinica – English Edition 90, 738–748.

Kershaw, A.P., D'Costa, D.M., McEwen Mason, J.R.C., Wagstaff, B.E., 1991. Palynological evidence for Quaternary vegetation and environments of mainland southeastern Australia. Quaternary Science Reviews 10, 391–404.

Khan, A.A., Kolattukudy, P.E., 1974. Decarboxylation of long chain fatty acids to alkanes by cell free preparations of pea leaves (*Pisum sativum*). Biochemical and Biophysical Research Communications 61, 1379–1386.

Koch, K., Dommisse, A., Niemietz, A., Barthlott, W., Wandelt, K., 2009. Nanostructure of epicuticular plant waxes: self-assembly of wax tubules. Surface Science 603, 1961–1968.

Koch, K., Neinhuis, C., Ensikat, H.J., Barthlott, W., 2004. Self assembly of epicuticular waxes on living plant surfaces imaged by atomic force microscopy (AFM). Journal of Experimental Botany 55, 711–718.

Leider, A., Hinrichs, K.-U., Schefuß, E., Versteegh, G.J.M., 2013. Distribution and stable isotopes of plant wax derived *n*-alkanes in lacustrine, fluvial and marine surface sediments along an Eastern Italian transect and their potential to reconstruct the hydrological cycle. Geochimica et Cosmochimica Acta 117, 16–32.

Li, R., Fan, J., Xue, J., Meyers, P.A., 2017. Effects of early diagenesis on molecular distributions and carbon isotopic compositions of leaf wax long chain biomarker n-alkanes: comparison of two one-year-long burial experiments. Organic Geochemistry 104, 8–18.

Lichtfouse, É., Chenu, C., Baudin, F., Leblond, C., Da Silva, M., Behar, F., Derenne, S., Largeau, C., Wehrung, P., Albrecht, P., 1998. A novel pathway of soil organic matter formation by selective preservation of resistant straight-chain biopolymers: chemical and isotope evidence. Organic Geochemistry 28, 411–415.

Macken, A.C., McDowell, M.C., Bartholomeusz, D.N., Reed, E.H., 2013. Chronology and stratigraphy of the Wet Cave vertebrate fossil deposit, Naracoorte, and relationship to paleoclimatic conditions of the Last Glacial Cycle in south-eastern Australia. Australian Journal of Earth Sciences 60, 271–281.

Makou, M., Eglinton, T., McIntyre, C., Montluçon, D., Antheaume, I., Grossi, V., 2018. Plant wax *n*-alkane and *n*-alkanoic acid signatures overprinted by microbial contributions and old carbon in meromictic lake sediments. Geophysical Research Letters 45, 1049–1057.

Marzi, R., Torkelson, B.E., Olson, R.K., 1993. A revised carbon preference index. Organic Geochemistry 20, 1303–1306.

Meyers, P.A., Hites, R.A., 1982. Extractable organic compounds in midwest rain and snow. Atmospheric Environment 16, 2169–2175.

Nelson, D.B., Knohl, A., Sachse, D., Schefuß, E., Kahmen, A., 2017. Sources and abundances of leaf waxes in aerosols in central Europe. Geochimica et Cosmochimica Acta 198, 299–314.
Nguyen Tu, T.T., Egasse, C., Anquetil, C., Zanetti, F., Zeller, B., Huon, S., Derenne, S., 2017. Leaf lipid degradation in soils and surface sediments: a litterbag experiment. Organic Geochemistry 104, 35–41.
Oades, J.M., 1988. The retention of organic matter in soils. Biogeochemistry 5, 35–70.
Pisani, O., Frey, S.D., Simpson, A.J., Simpson, M.J., 2015. Soil warming and nitrogen deposition alter soil organic matter composition at the molecular-level. Biogeochemistry 123, 391–409.
Pu, Y., Zhang, H., Wang, Y., Lei, G., Nace, T., Zhang, S., 2011. Climatic and environmental implications from *n*-alkanes in glacially eroded lake sediments in Tibetan Plateau: an example from Ximen Co. Chinese Science Bulletin 56, 1503–1510.
Quenea, K., Derenne, S., Largeau, C., Rumpel, C., Mariotti, A., 2004. Variation in lipid relative abundance and composition among different particle size fractions of a forest soil. Organic Geochemistry 35, 1355–1370.
Quénéa, K., Largeau, C., Derenne, S., Spaccini, R., Bardoux, G., Mariotti, A., 2006. Molecular and isotopic study of lipids in particle size fractions of a sandy cultivated soil (Cestas cultivation sequence, southwest France): sources, degradation, and comparison with Cestas forest soil. Organic Geochemistry 37, 20–44.
R Core Team, 2018. R: A Language and Environment for Statistical Computing. R Foundation for Statistical Computing, Vienna, Austria. <https://www.R-project.org/>.
Rommerskirchen, F., Eglinton, G., Dupont, L., Rullkötter, J., 2006. Glacial/interglacial changes in southern Africa: compound-specific $\delta^{13}C$ land plant biomarker and pollen records from southeast Atlantic continental margin sediments. Geochemistry, Geophysics, Geosystems 7. https://doi.org/10.1029/2005GC001223.
Rouillard, A., Greenwood, P.F., Grice, K., Skrzypek, G., Dogramaci, S., Turney, C., Grierson, P.F., 2016. Interpreting vegetation change in tropical arid ecosystems from sediment molecular fossils and their stable isotope compositions: a baseline study from the Pilbara region of northwest Australia. Palaeogeography, Palaeoclimatology, Palaeoecology 459, 495–507.
Sachse, D., Radke, J., Gleixner, G., 2004. Hydrogen isotope ratios of recent lacustrine sedimentary *n*-alkanes record modern climate variability. Geochimica et Cosmochimica Acta 68, 4877–4889.
Schwark, L., Zink, K., Lechterbeck, J., 2002. Reconstruction of postglacial to early Holocene vegetation history in terrestrial Central Europe via cuticular lipid biomarkers and pollen records from lake sediments. Geology 30, 463–466.
Shepherd, T., Wynne Griffiths, D., 2006. The effects of stress on plant cuticular waxes. New Phytologist 171, 469–499.
Smith, F.A., Wing, S.L., Freeman, K.H., 2007. Magnitude of the carbon isotope excursion at the Paleocene-Eocene thermal maximum: the role of plant community change. Earth and Planetary Science Letters 262, 50–65.
Smittenberg, R.H., Eglinton, T.I., Schouten, S., Sinninghe Damsté, J.S., 2006. Ongoing buildup of refractory organic carbon in boreal soils during the Holocene. Science 314, 1283–1286.
Tipple, B.J., Pagani, M., 2013. Environmental control on eastern broadleaf forest species' leaf wax distributions and D/H ratios. Geochimica et Cosmochimica Acta 111, 64–77.
van Gardingen, P.R., Grace, J., Jeffree, C.E., 1991. Abrasive damage by wind to the needle surfaces of *Picea sitchensis* (Bong.) Carr. and *Pinus sylvestris* L. Plant, Cell & Environment 14, 185–193.
Wang, C., Eley, Y., Oakes, A., Hren, M., 2017a. Hydrogen isotope and molecular alteration of n-alkanes during heating in open and closed systems. Organic Geochemistry 112, 47–58.
Wang, C., Hren, M.T., Hoke, G.D., Liu-Zeng, J., Garzione, C.N., 2017b. Soil *n*-alkane δD and glycerol dialkyl glycerol tetraether (GDGT) distributions along an altitudinal transect from southwest China: evaluating organic molecular proxies for paleoclimate and paleoelevation. Organic Geochemistry 107, 21–32.
White, A., Sparrow, B., Leitch, E., Foulkes, J., Flitton, R., Lowe, A., Caddy-Retalic, S., 2012. AusPlots Rangelands Survey Protocols Manual, Terrestrial Ecosystem Research Network. University of Adelaide Press, University of Adelaide, p. 84.
Wright, I.J., Cannon, K., 2001. Relationships between leaf lifespan and structural defences in a low-nutrient, sclerophyll flora. Functional Ecology 15, 351–359.
Wright, I.J., Reich, P.B., Westoby, M., Ackerly, D.D., Baruch, Z., Bongers, F., Cavender-Bares, J., Chapin, T., Cornelissen, J.H.C., Diemer, M., Flexas, J., Garnier, E., Groom, P.K., Gulias, J., Hikosaka, K., Lamont, B.B., Lee, T., Lee, W., Lusk, C., Midgley, J.J., Navas, M.-L., Niinemets, U., Oleksyn, J., Osada, N., Poorter, H., Poot, P., Prior, L., Pyankov, V.I., Roumet, C., Thomas, S.C., Tjoelker, M.G., Veneklaas, E.J., Villar, R., 2004. The worldwide leaf economics spectrum. Nature 428, 821–827.
Xu, T., Hutchinson, M.F., 2013. New developments and applications in the ANUCLIM spatial climatic and bioclimatic modelling package. Environmental Modelling & Software 40, 267–279.
Yamamoto, S., Hasegawa, T., Tada, R., Goto, K., Rojas-Consuegra, R., Díaz-Otero, C., García-Delgado, D.E., Yamamoto, S., Sakuma, H., Matsui, T., 2010. Environmental and vegetational changes recorded in sedimentary leaf wax n-alkanes across the Cretaceous-Paleogene boundary at Loma Capiro, Central Cuba. Palaeogeography, Palaeoclimatology, Palaeoecology 295, 31–41.
Yamamoto, S., Kawamura, K., 2010. Compound-specific stable carbon and hydrogen isotopic compositions of *n*-alkanes in urban atmospheric aerosols from Tokyo. Geochemical Journal 44, 419–430.
Zaleha, M.J., 1997. Siwalik Paleosols (Miocene, northern Pakistan); genesis and controls on their formation. Journal of Sedimentary Research 67, 821–839.
Zech, M., Pedentchouk, N., Buggle, B., Leiber, K., Kalbitz, K., Marković, S.B., Glaser, B., 2011. Effect of leaf litter degradation and seasonality on D/H isotope ratios of *n*-alkane biomarkers. Geochimica et Cosmochimica Acta 75, 4917–4928.